minerals

MDPI

Article

Salinity Effects on the Physicochemical and Mechanical Behavior of Untreated and Lime-Treated Saline Soils

Imed Benrebouh [1], Ilyas Hafhouf [2], Abdellah Douadi [2], Abdelghani Merdas [1], Abderrahim Meguellati [1] and Paulina Faria [3,*]

[1] Emergent Materials Research Unit (EMRU), Department of Civil Engineering, University Ferhat Abbas Setif 1, Setif 19000, Algeria; imed.benrebouh@univ-setif.dz (I.B.); abdelghani.merdas@univ-setif.dz (A.M.); abderrahim.meguellati@univ-setif.dz (A.M.)

[2] Civil Engineering Research Laboratory of Setif (LRGCS), Department of Civil Engineering, Ferhat Abbas University of Setif 1, Setif 19000, Algeria; ilyas.hafhouf@gmail.com (I.H.); abdellah.douadi@univ-setif.dz (A.D.)

[3] CERIS, Department of Civil Engineering, NOVA School of Science and Technology, NOVA University Lisbon, 2829-516 Caparica, Portugal

* Correspondence: paulina.faria@fct.unl.pt

Abstract: Improving saline soils' properties by incorporating limes is a practical technique, generally due to cation exchange, pozzolanic reaction, and carbonation. This study explores how soil salinity, measured by electrical conductivity, affects untreated and lime-treated saline soils. An Algerian sebkha soil (from Ain M'lila) with an original high salinity (ECe3 = 23.2 dS.m^{-1}) was used. The same soil was washed to create medium (ECe2 = 8.3 dS.m^{-1}) and low (ECe1 = 2.32 dS.m^{-1}) salinity soil samples. The results of this study indicate that salinity influenced the shape of the particle size distribution curve, particularly in the silt range. Salinity also had a significant effect on carbonate content ($CaCO_3$) and unconfined compressive strength (UCS). For the untreated soil, when salinity decreased, the UCS and $CaCO_3$ content increased. However, when salinity decreased for the treated soil, the UCS increased, while the $CaCO_3$ content decreased. X-ray diffraction (XRD) analysis of untreated soils showed halite (NaCl) disappearance and gypsum ($CaSO_4$ $2H_2O$) reduction with decreasing salinity in ECe1. In treated soil at ECe3, these mineral phases remained constant. While XRD detected no new cementitious phases in treated ECe3 or ECe1 samples, thermogravimetric analysis confirmed the presence of portlandite in both. As Ain M'lila sebkha is a chloride–sulfate soil, the dissolution of the halite and gypsum phases released more Cl^- and SO_4^{2-} ions into the interstitial solution. In a low fraction of clay, these ions obstructed and slowed the pozzolanic reaction in the ECe3 soil. Identifying the season when this type of soil has lower salinity can be beneficial for treatment from a technical, economic, and environmental point of view.

Keywords: Ain M'lila sebkha soil; building lime; chloride–sulfate soil; salt content; soil treatment; unconfined compressive strength

check for updates

Citation: Benrebouh, I.; Hafhouf, I.; Douadi, A.; Merdas, A.; Meguellati, A.; Faria, P. Salinity Effects on the Physicochemical and Mechanical Behavior of Untreated and Lime-Treated Saline Soils. *Minerals* **2024**, *14*, 1217. https://doi.org/10.3390/min14121217

Academic Editor: Carlos Sierra Fernández

Received: 23 October 2024
Revised: 21 November 2024
Accepted: 26 November 2024
Published: 28 November 2024

Copyright: © 2024 by the authors. Licensee MDPI, Basel, Switzerland. This article is an open access article distributed under the terms and conditions of the Creative Commons Attribution (CC BY) license (https://creativecommons.org/licenses/by/4.0/).

1. Introduction

Sebkha soils are saline soils containing salts that are hygroscopic, soluble in and transported by water. These soils develop in regions where evaporation rates exceed rainfall. The salinity of sebkha is mainly influenced by natural conditions such as drying–wetting cycles. When sebkha comes into contact with water, soluble salts dissolve and are moved downward by gravity, resulting in lower salinity. However, the effects of evaporation of groundwater cause salts to move upward, increasing soil salinity. According to Liu et al. [1], soil salinity variation is a critical factor that requires special attention in the construction of civil engineering projects. It induced significant degradation in these projects, such as differential settlement [2], collapses [3–5], and strength losses [4,6].

Several researchers have studied the effect of salinity on the physicochemical and mechanical properties of soils [7–11]. Their findings indicated that the degree of salinity's influence varied significantly based on soil type, salt type, and salt content. According to a study by Xiao-hua et al. [12], coarse-grained soil's physical and mechanical characteristics correlated with particle structure and salt concentration. Velde and Meunier [13] demonstrated that increasing the salinity of irrigation water led to the breakdown of soil aggregates via swelling and dispersion of clay platelets, resulting in a loose soil structure. Mohammed and Abdullah [14] found that increasing water salinity significantly decreased the clay fraction in fine soils, with the reduction varying by soil type. Saline soils consistently have a lower clay fraction than nonsaline soils. The consolidating effect of salts, namely from sea water rich in sodium chloride (NaCl), can be also observed on simple earthen constructions built for human consumption where NaCl is produced naturally by the seaside [15]. However, although the use of and research into earth extracted from the soil is increasing because of environmental issues [16], saline soils are frequently rejected from this use. Therefore, it is important to find ways to improve the mechanical performance of earthen building products produced with this type of soil, as well as their durability [17].

The salinity of sebkha soil decreased from 16.3 $dS.m^{-1}$ to 3.8 $dS.m^{-1}$ because of leaching of ions from soluble salts such as halite and gypsum [18]. Ying et al. [19] confirmed that the salinity had a significant effect on the water retention capacity. A recent study conducted by Li and Yang [20] showed that an increase in chloride content led to the formation of more particle agglomerates in the soil. However, an excess of salt content changed the soil structure and reduced its resistance. Shen et al. [8] demonstrated that increased $NaHCO_3$ content led to higher liquidity and plasticity limits but reduced mechanical properties. This adverse impact was also supported by Nu et al. [7], who found that higher salinity in soft soil resulted in lower shear strength and increased liquid limit. Zhang et al. [21] also showed that higher salinity decreased resistance.

Based on the results of the aforementioned studies, several techniques have been implemented in recent years to improve the physicochemical and mechanical characteristics of saline soils. These include the leaching technique to reduce salt content, the use of geotextiles as insulation layers, and the incorporation of mineral binders, such as air lime [1,22,23]. However, the latter technique is widely favored in road construction for its reliability, low costs, and exceptional strength [24–26]. Determining the optimum lime content (OLC) is crucial for construction projects. The Eades and Grim pH method [27] defines OLC as the lime amount yielding the highest solution pH. However, this method is affected by ions from lime and soil, and research on the influence of soluble soil ions on pH values is still limited. In this respect, Emarah and Seleem [28] found that adding hydrated lime to soil treated with Red Sea water raised the suspension's pH linearly, stabilizing at 3%–4% lime content. Beyond this point, the pH continued to increase with additional lime content. On the other hand, a strong correlation between OLC and salinity was observed in a study conducted by Ying et al. [11]. The OLC levels were 1.5%, 3%, and 4% by dry weight for the deionized water–quick lime, synthetic seawater–quick lime, and mixed salt solution–quick lime suspensions. Recently, several researchers [1,4,29] have been investigating the use of lime to treat saline soils. According to Moayed et al. [4], saline soils can be used as a subbase for flexible pavements, because adding 2% hydrated lime led to an almost twofold increase in UCS after 7 d compared with untreated soil. Pei and Shouxi [30] investigated the potential use of saline soil from the Gulf of Bohai as a material for filling roads. They concluded that the soil's UCS improved significantly after adding lime, making it suitable for road construction. Previous research conducted by Jiang et al. [31] and Wei et al. [32] also noted increases in soil strength when Portland cement and hydrated lime were added. However, several researchers have shown that the negative effect of salts remains after adding a hydraulic or aerial binder [33–37]. Koslanant [33] concluded that the increase in soil strength after increasing salinity is attributable to the coagulation of organic matter in these soils by salts, which encourages clay particles to react

with the hydraulic binder. Zhang et al. [34] showed that after 28 days of curing, the UCS of soil treated with 10% cement decreased by 33% from 0.27 MPa to 0.18 MPa when the salt content increased from 2.5% to 5%. Soluble salt ions negatively impacted the cementing bonding between the soil particles. Li et al. [37] found that adding 8% chloride salt (Cl^-) to a lime-treated chloride soil decreased UCS by 50% after 28 days. While Cl^- ions do not participate in hydration, they are adsorbed onto soil pores and surfaces. Xing et al. [35] conducted tests on salt-rich soil treated with a cement, including UCS and X-ray diffraction tests. Their findings indicated that the strength of the treated soil was not enhanced. This was attributed to the presence of Cl^- and Mg^{2+}, which hinder the formation of CSH and CAH, thereby preventing soil strength improvement. Research conducted by Cuisinier et al. [38] and Carteret et al. [39] indicated that Cl^- negatively impacted the resistance of treated soils in the short and long term. Furthermore, $SO_4{}^{2-}$ ions negatively impacted the mechanical properties of treated soil by reacting with Al^{3+} and Ca^{2+} ions. This reaction produced ettringite, an expansive phase that disrupts the soil structure and decreases its resistance [34,35,40]. In addition, a study carried out by Rica et al. [41] on the disruptive effects of salts on treated silty soil deduced that the presence of combinations of salts with $SO_4{}^{2-}$ ions aggravated the latter's deleterious effects on the treated soil.

The studies mentioned above indicate that the nature of the soil, salt, and salt content could negatively affect the physicochemical and mechanical behavior of saline soils without or with treatment by binder addition. It is essential to note that most of these studies have generally investigated the effect of a single type of salt. In contrast, in natural field conditions, interactions between several types of salt are more likely to occur. Moreover, studies conducted by Nie et al. [42] and Zhang et al. [43] indicated that the structure of soil containing at least 10% clay was significantly influenced by the chemical environment of the pore solution. However, with high evaporation in summer, a significant quantity of salts is generally produced in the sebkha system.

Algeria has 254 sebkha zones and has revealed substantial economic growth in recent years [44]. The high plains have a semiarid climate and contain approximately 20 sebkha areas [45]. One of these areas is the sebkha of Ain M'lila (Ez Zemoul). This sebkha experiences winter rainfall, reducing soil salinity, with salinity also decreasing horizontally from the edges toward the center. However, increased civil engineering projects, such as roads and railways, have strained these virgin areas. Notably, the intersection of the National Road RN03 with the sebkha has caused issues such as cracks and subsidence. To prevent similar problems in future projects, the present study was conducted, aiming to examine the impact of salinity (natural types of salt and different levels found in the soil) on the physical, chemical, and mechanical properties of untreated and binder-treated sebkha soil in Ain M'lila. This study involved physical tests using granulometric analysis; mechanical tests, including UCS; chemical tests via calcimeter and XRF; and mineralogical tests, including XRD and TGA.

2. Materials and Methods

2.1. Materials

2.1.1. Study Area

The study site (Figure 1), known in Arabic as Lake Mezouri or Sebkha Ez Zemoul, is located 13.5 km south of Ain M'lila town and 10.5 km east of the town of Souk Naaman in the province of Oum el Bouaghi in northeast Algeria. The sebkha covers an area of around 61 km^2 and is located at 35°53′ N, 06°30′ E, at an altitude of 784 m above sea level [46], and it was classified as one of the Mediterranean Ramsar sites in 2004.

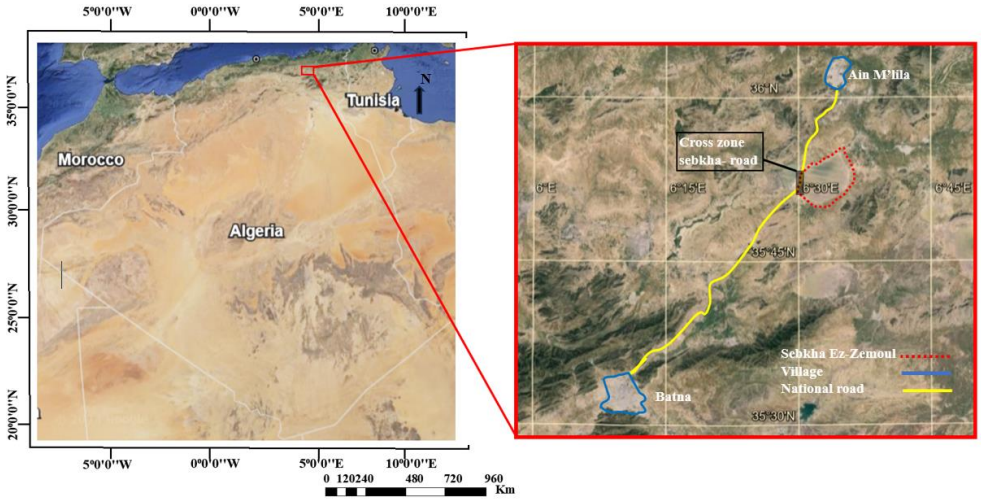

Figure 1. Ain M'lila sebkha soil location.

Meteorological data from the Constantine region (approximately 40 km a way) shows an annual rainfall of 700 mm, with 77% occurring between December and April. The evaporation rate is approximately 1013 mm [46], nearly 1.5 times the rainfall, leading to a distinctive white layer on the sebkha's surface (Figure 2a). A zoom in on the open survey state (Figure 2b) indicates that the sebkha profile revealed that it contains sand, silt, and clay (Figure 2c). However, this study was limited to the dry areas along the RN03 because of the high salinity levels compared with inside the sebkha. In addition, the runoff from the sewerage systems of the town of Souk Naaman renders access to these wet areas of the sebkha soil difficult. In summer, the surface of the sebkha develops a white crust with high solubility, indicating the presence of halite minerals. In contrast, deeper in the sedimentary profile, gypsum crystals with low solubility were found (Figure 2d). To this end, the summer season and the edge of the sebkha (all along the RN03) were chosen for collecting samples, following the procedure described by Aiban et al. [22] (i.e., excluding pieces of salt crystals).

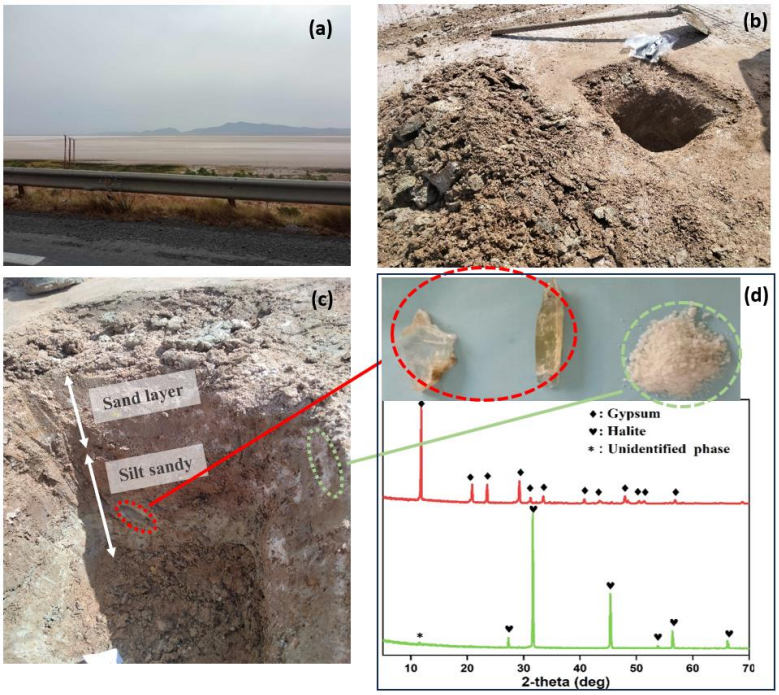

Figure 2. Ain M'lila sebkha soil: (**a**) white layer on sebkha's surface; (**b**) sky survey state; (**c**) sebkha profile; (**d**) mineralogy of soluble salts.

2.1.2. Soil and Lime Characteristics

Some geotechnical characteristics of the sebkha soil are presented in Table 1. The maximum dry density was γ_{dopn} = 1.841 g/cm^3, corresponding to the optimum water content of w_{opt} = 11.8%, obtained according to standard NF P94-093 [47]. The particle size distribution, determined by dry sieving and sedimentation methods, revealed that the silt content (66%) was the highest, followed by sand (26%) and clay (10%). In addition, the plastic limit (Pl) and index (PI) were 16.51% and 16.49%, respectively. According to the USCS soil classification system, the soil is classified as sandy silt clay (CL). However, textural classification suggests it should be classified as silt loam [48].

Table 1. Geotechnical characteristics of sebkha soil.

Soil's Parameters (Unit)	Value	Methods
Case: Intact soil		
Unconfined compressive strength UCS (kPa)	33	[49]
Natural water content w_{nat} (%)	18.19	[50]
Maximum dry density γ_{dopn}	1.841	[47]
Optimum moisture content w_{opt} (%)	11.8	
≤2 mm fraction (%)	100	[51]
≤80 µm fraction (%)	76	
≤2 µm fraction (%)	10	[52]
Plastic limit PL (%)	16.51	[53]
Plastic index PI (%)	16.49	
USCS classification	CL	[54]
$CaCO_3$ content (%)	31.3	[55]

The saturated soil paste extract method was used to measure the soil's salinity and primary soluble salt content (Table 2). A salinity value of 23.2 dS.m^{-1} was determined, indicating that the soil was highly saline according to the U.S. Salinity Laboratory Staff [56]. In addition, the soil was classified as a neutral chloride–sulfate saline soil based on the high content of chloride (6874 mg/L) and sulfate (5605 mg/L) species present as soluble salts [57]. Moreover, the results of the X-ray fluorescence analysis, shown in the histogram of Figure 3a, indicated that the main chemical composition of the soil was silica (SiO_2), followed by calcium oxide (CaO), alumina (Al_2O_3), and magnesium oxide (MgO), while sodium (Na_2O), sulfate (SO_3), ferrite (Fe_2O_3), chloride (Cl), and potassium oxide (K_2O) all existed in small quantities. In addition, X-ray diffraction analysis (Figure 3b) revealed that the soil contained quartz, calcite, halite, gypsum, and kaolinite. The mineralogical results, verified against the ICDD Powder Diffraction File database, aligned with the chemical findings. These results indicated the presence of quartz (PDF Card No. 01-078-1254) and kaolinite (PDF Card No. 01-072-2300) in the silica and alumina, calcite (PDF Card No. 00-017-0763) and gypsum (PDF Card No. 00-006-0046) in the calcium oxide, and halite (PDF Card No. 01-088-2300) in the chloride.

Table 2. The chemical compositions obtained based on the saturated soil past extract: salinity, salt concentration, pH, and soluble salt content.

ECe (dS.m^{-1})	Salt Concentration (g.L^{-1})	pH	Soluble Salt Content (mg.L^{-1})						
			Ca^{2+}	Mg^{2+}	Na^+	K^+	SO_3^-	Cl^-	HCO_3^-
23.2	17.64	6.81	466.1	172.3	4452	56	5605	6874	12

This study utilized quicklime (CaO > 83.3%) (see Table 3) as a dry, white powder sourced from Saida province in western Algeria. This powder was stored in plastic bags to prevent contact with moisture, hydration, and carbonation.

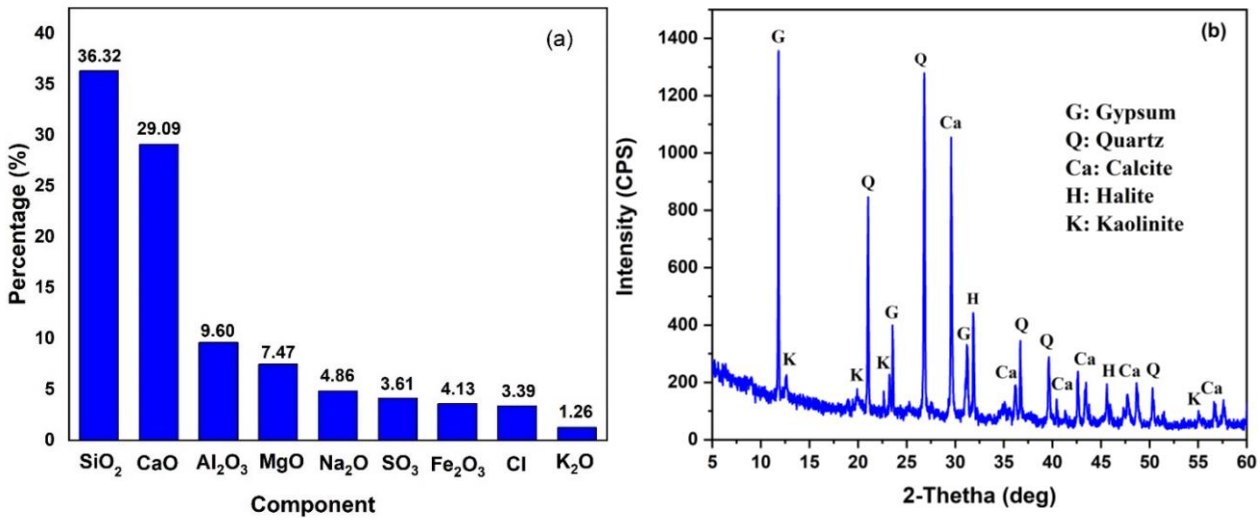

Figure 3. Chemical composition by XRF (**a**) and mineralogical composition by XRD (**b**) of sebkha soil ECe3.

Table 3. Chemical composition of lime.

Physical State	Specified Density	>90 µm Fraction (%)	Chemical Elements (%)						
Dry, white powder	2	<90	CaO >83.3	SiO_2 <2.5	Fe_2O_3 <2.0	Al_2O_3 <1.5	MgO <0.5	SO_3 <0.5	Na_2O 0.4–0.5

2.2. Methods

2.2.1. Soil Sampling and Preparation

On 4 October 2021, three open pit survey holes were excavated along RN03 using a handle shovel at depths ranging from 0 to 1 m. The soil was collected and oven dried at 50 °C because of its sensitivity to heat. The samples were then lightly crushed with a plastic hammer to break the natural cementing bonds between the soil particles. However, some salt crystals and soil aggregates were still visible (Figure 4a), so this process was repeated until all the material had passed through a 2 mm opening sieve. The dry-sieved samples were divided into three parts. The unwashed part consisted of highly saline soil (ECe3 = 23.2 dS.m^{-1}). In contrast, the other parts were washed separately with demineralized water (D-W) to create two groups of samples with different salinities: moderately saline soil (ECe2 = 8.3 dS.m^{-1}) and slightly saline soil (ECe1 = 2.32 dS.m^{-1}). The washing process is illustrated in Figure 4b. The sebkha was washed with D-W using a cylindrical steel bar. After washing, the mixture was left to stand for 24 h before the clear water was removed using a plastic tube based on the gravimetric method. The oven-dried sebkha soils with three different salinities were then crushed and sieved.

The salinity levels of each soil were tested to determine their OLCs. pH tests following the pH method [27] were conducted initially to minimize the required tests for the continuing experimental program for the treated samples with the addition of 1%, 2%, 3%, 4%, and 5% (in mass) of lime. The results of these tests are shown in Figure 5.

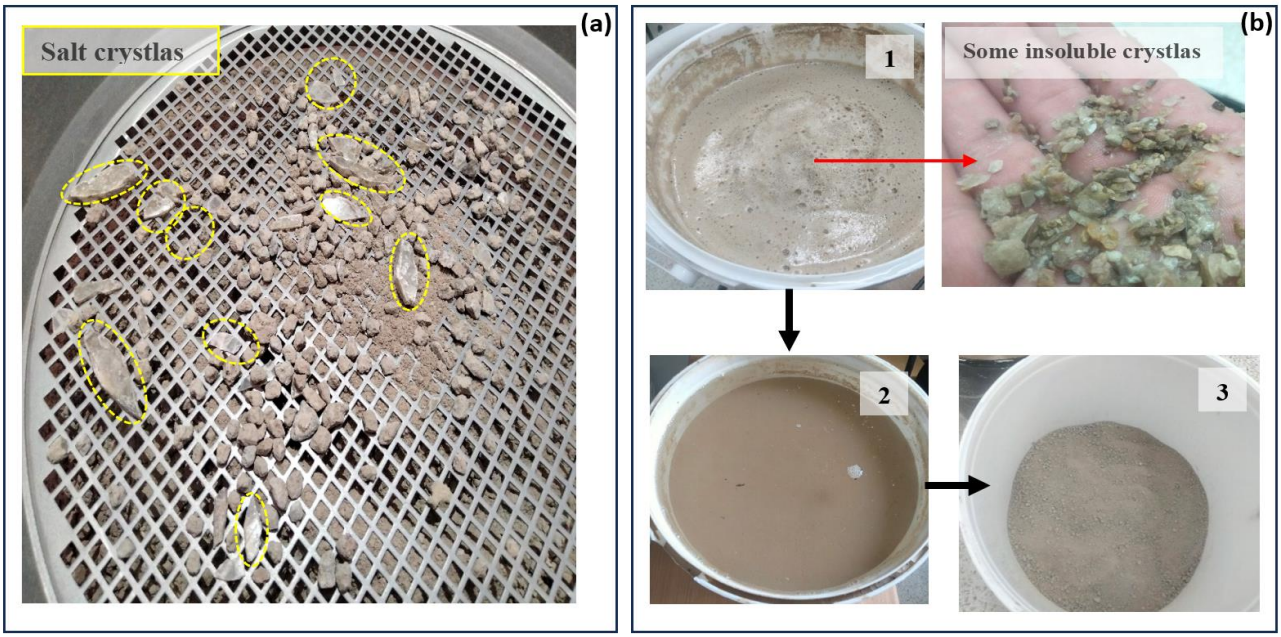

Figure 4. Sample preparation: (**a**) soil crystals and aggregates; (**b**) washing process by numerical order.

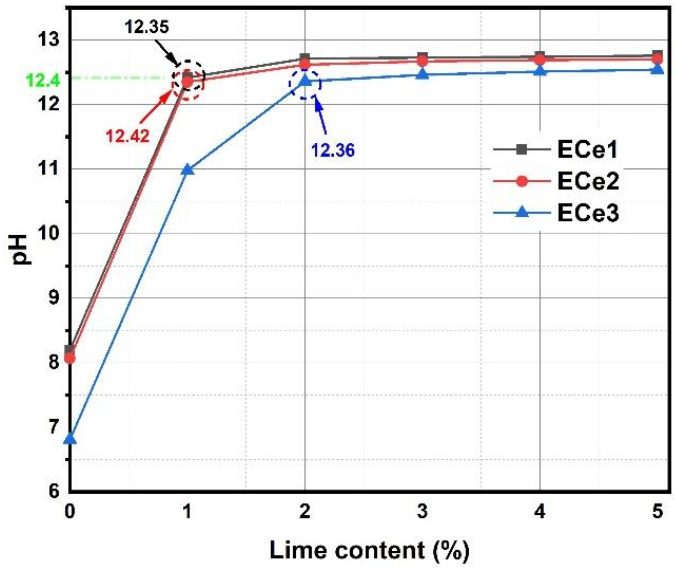

Figure 5. Lime and salinity impact on the pH of solutions.

Before adding lime, the pH of the natural soil, ECe3, was lower (6.81) than that of ECe1 and ECe2 (8.05 and 8.2, respectively) because of increased salinity. According to a study by Thomas [58], in a saline soil solution, if the negative charge of the ions exceeds the positive charge, the pH decreases because of the release of more H^+ than OH^-. As shown in Table 2, in the present study, for the natural soil ECe3, the total charge of anions (negative charge) was greater than that of cations (positive charge) (8299 mg/L vs. 2920.7 mg/L). It is also important to note that the decrease in salinity for ECe1 and ECe2 soils after the washing operations reduced the total negative charge because of the leaching of halite and some gypsum. This reduction explains the increase in pH with the decrease in salinity of the Ain M'lila sebkha soil. The pH levels increased when lime was added to the different soil types. The increase was more pronounced for the ECe1 soil than the ECe2 and ECe3 soils, as the lime content varied from 1% to 5%. After adding 1% of lime, the pH values for the ECe1 and ECe2 soils rapidly rose to 12.42 and 12.35, respectively.

These values then slightly increased to 12.76 and 12.70, respectively, after adding 5% of lime. However, for soil ECe3, the pH value increased considerably up to 2% lime content and then only slightly, from 12.46 to 12.56, as the lime content varied between 3% and 5%. According to several studies [27,59–61], the OLC is the minimum amount needed to achieve the highest pH in a soil–lime–water mixture. Based on previous research and the present study findings, the OLC for ECe1 and ECe2 soils was 1%, while for ECe3 soil, it was 2%. Hence, higher salinity levels require a higher OLC. The pH values for this ECe3 soil were expected to be lower than for ECe2 and ECe1 soils because of the consumption of OH- released by Mg^{2+} and Ca^{2+} ions in the saline solution inducing the precipitation of $Mg(OH)_2$ and $CaCO_3$, causing greater lime consumption [11]. To ensure that the three saline soils contained sufficient quantities of Ca^{2+} for a pozzolanic reaction during curing and to create a favorable alkaline environment for this reaction, higher dosages of lime (1.5% for the ECe1 and ECe2 soils and 3% for the ECe3 soil) were selected, and supplementary specimens were prepared for the UCS tests.

The following steps were carried out for each group of samples: the soil, lime, and water were thoroughly mixed for approximately three minutes at medium speed using an automated mixer. The mixture was then sealed in plastic bags for 24 h. Each sample consisted of three layers, each being compacted at a constant speed of 1.27 mm/min using the CBR mold and machine until they reached 95% of the dry density obtained in the standard Proctor tests (e.g., 1.749 g/cm^3 for the untreated samples). Before each sample was preserved in a climatic chamber (relative humidity = 90 ± 2% and T = 20 ± 2 °C), it was wrapped in plastic film and paraffin after checking the mass tolerance by weighing to two decimal places (0.01 g).

2.2.2. Chemical, Mineralogical, and Geotechnical Tests

The carbonate ($CaCO_3$) content in each soil sample was determined using the volumetric method specified in standard NF P 94-048 [55]. This method involved shaking 10 mL of 37% diluted hydrochloric acid (HCl) with 1 g of soil sample sieved to 0.2 mm. As a result, the soil dissolved and released CO_2, causing a decrease in the water level in a graduated tube. It is important to note that the dissolution of 4 mg of $CaCO_3$ corresponds to the release of 1 cm^3 of CO_2, based on the chemical Equation (1) for the reaction:

$$CaCO_3 + 2HCl \rightarrow CaCl_2 + H_2O + CO_2 \quad (1)$$

A Dietrich–Frühling calcimeter (Figure 6) was used for this process.

The mineralogical composition of this soil was determined by X-ray diffraction (XRD) after pulverizing soil samples. This analysis used a Siemens D500 powder diffractometer (Malvern, UK) and a Bruker AXS (Karlsruhe, Germany) model equipped with a nickel anticathode (Kα = 1.5406 Å) connected to a microcomputer for data collection and processing. The X-ray tube settings were 20 mA and 30 kV.

The elemental chemical composition of the sebkha soil was analyzed by X-ray fluorescence spectrometry (XRF) using a Rigaku ZSX Prisus IV instrument (Tokyo, Japan). XRF is a semiquantitative analytical technique used to determine the concentration of chemical elements in powdered soil samples. In addition, soil pH was measured based on soil extract 1/2.5. However, electrical conductivity (EC) was measured using an Inolab-Cond conductivity meter (WTW 1CA301) (Troyes, France) to assess soil salinity based on the diluted soil extract method (1/5). This method provided the salinity of the soluble salts in the pore water, quantified in dS.m^{-1}. The cations and anions of various soluble salts were determined using the volumetric measurement methods detailed by Pansu and Gautheyrou [62].

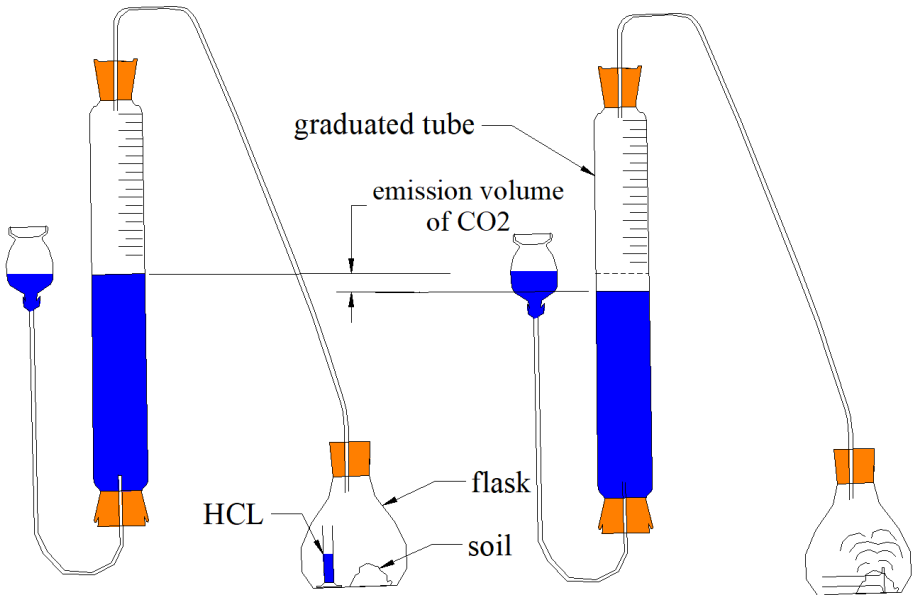

Figure 6. Dietrich–Frühling calcimeter.

A model SDT Q600 equipment (TA Instrument) (New Castle, DE, USA) was used for thermogravimetric analysis (TGA). This instrument was connected to a computer system for data acquisition and processing. Each platinum crucible contained 35 mg of ground soil. The samples were heated at 10 °C/min from 20 to 950 °C while exposed to a flow of 99.99% pure argon at 50 mL/min.

The geotechnical properties of the soil, including particle size analysis and Atterberg limits, were determined following the standards NF P 94-056 [51], NF P 94-057 [52], and ASTM D4318-00 [53]. Standard Proctor compaction tests were conducted per NF P 94-093 [47].

2.2.3. Unconfined Compressive Strength Test

The unconfined compressive strength (UCS) test was performed using a Zwick testing machine (Ulm, Germany) following the NF P 94-077 [49] standard. Specimens from the humid chamber were unsealed from the plastic film and quickly placed (to inhibit moisture evaporation) on the lower platen, and the movable upper platen made contact with it. A 1 mm/min displacement speed was used, which equaled approximately 1.66% of the specimen's height per minute. Data were collected using a computer connected to the system, and the maximum force and corresponding failure strain were recorded for each axial force–strain curve. The UCS was determined by the ratio of the maximum axial force (F) to the average cross-sectional area of the sample (A) (Equation (2)):

$$\mathrm{UCS} = {}^{\mathrm{F}}/_{\mathrm{A}} \quad \text{and} \quad \mathrm{A} = {}^{\mathrm{A_0}}/_{(1-\varepsilon_l)} \tag{2}$$

A_0 represents the initial mean cross-sectional area, and ε_l represents the axial deformation caused by the applied force. The result was the average of three triplicate specimens.

3. Results and Discussion

3.1. Effect of Salinity on Carbonation Content of Untreated Sebkha Soil

Figure 7 illustrates the impact of salinity on the calcium carbonate ($CaCO_3$) content of untreated samples at various salinity levels. The results demonstrate that soil salinity significantly affected the $CaCO_3$ content, with higher soil salinity led to lower measured $CaCO_3$ content. In the ECe3 soil, the $CaCO_3$ content was 41.58%, while in the ECe2 and ECe1 soils, it was 43.05% and 43.51%, respectively. The mineralogical characterization of the collected sebkha soil (ECe3) showed that halite and gypsum were the predominant

minerals in the saline phase. The chemical composition of this soil revealed a CaO content of 29.7%.

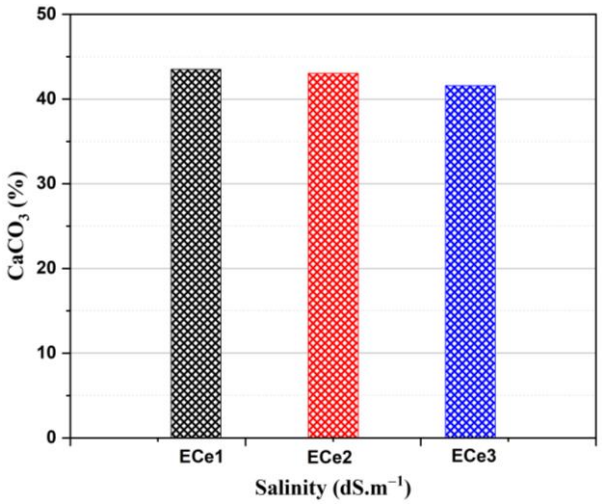

Figure 7. $CaCO_3$ content of ECe1, ECe2, and ECe3 soil by calcimeter.

According to Klein and Hurlbut [63], gypsum ($CaSO_4$, $2H_2O$) contains 32.6% calcium oxide (CaO), 46.5% sulfur trioxide (SO_3), and 20.9% combined water (H_2O). Since the ECe3 soil contained a large amount of gypsum, and gypsum contains almost 1/3 CaO of its total mass, more calcium cations would be captured by the sulfate anions. Thus, a greater decrease in the salinity of the ECe3 soil would result in a higher dissolution of gypsum, thereby providing greater availability of Ca^{2+} within the system. These Ca^{2+} ions may then react with the dissolved CO_2 present in the interstitial water, inducing the precipitation of $CaCO_3$. Consequently, the ECe1 soil, which had a greater availability of Ca^{2+} ions (i.e., a lower salinity), was characterized by a high $CaCO_3$ content. The XRF results also confirmed that the amount of sulfate continued to decrease after washing, leading to higher precipitation of CaO_3 content in the ECe1 soil than in the ECe3 soil, as illustrated in equation (3):

$$Ca^{2+} + CO_3^{2-} \rightarrow CaCO_3 \downarrow \quad (3)$$

The decrease in salinity to ECe1 in Ain M'lila sebkha soil led to an increase in the precipitation of $CaCO_3$ due to the decrease in sulfate.

3.2. Effect of Salinity on the Granulometry and Mineralogy of the Untreated Sebkha Soil

In order to study the effect of salinity on the particle size, chemical composition, and mineralogy of the sebkha soil, as mentioned before, a washing operation was conducted. The particle size curves obtained for each salinity level are illustrated in Figure 8a.

The latter shows the effect of salinity level on the shape of these curves. It was observed that salinity affected the silty fraction much more than the other fraction of the soil. The granulometric curves showed a nonconvergent trend in the range of silt grain sizes. This trend was more pronounced between the ECe1 and ECe3 soils. In ECe1 and ECe3 soils, 75% of the grains passed through the 80 µm sieve opening. Additionally, 56% and 38% of the grains in ECe1 and ECe3 soils had diameters of less than 20 µm, showing a difference of 18%. This difference suggests the influence of saline mineral phases in binding and agglomerating soil particles, thereby impacting the particle size distribution. These saline mineral phases increase the binding bridges and induce the cementation of particles with smaller specific surface areas, resulting in larger agglomerates and reduced finer particles. Leaching dissolved the weak cementitious bond between agglomerates, particularly the solubility of halite and some gypsum, resulting in finer particles in ECe1 soil than in ECe3 soil. On the other hand, Li and Yang [20] found that an increase in chlorine salt content was associated with a significantly higher number of agglomerates in the soil. However,

in the present study, the effect of salt was not observable in clay-sized particles, probably because of their low content (i.e., 10%).

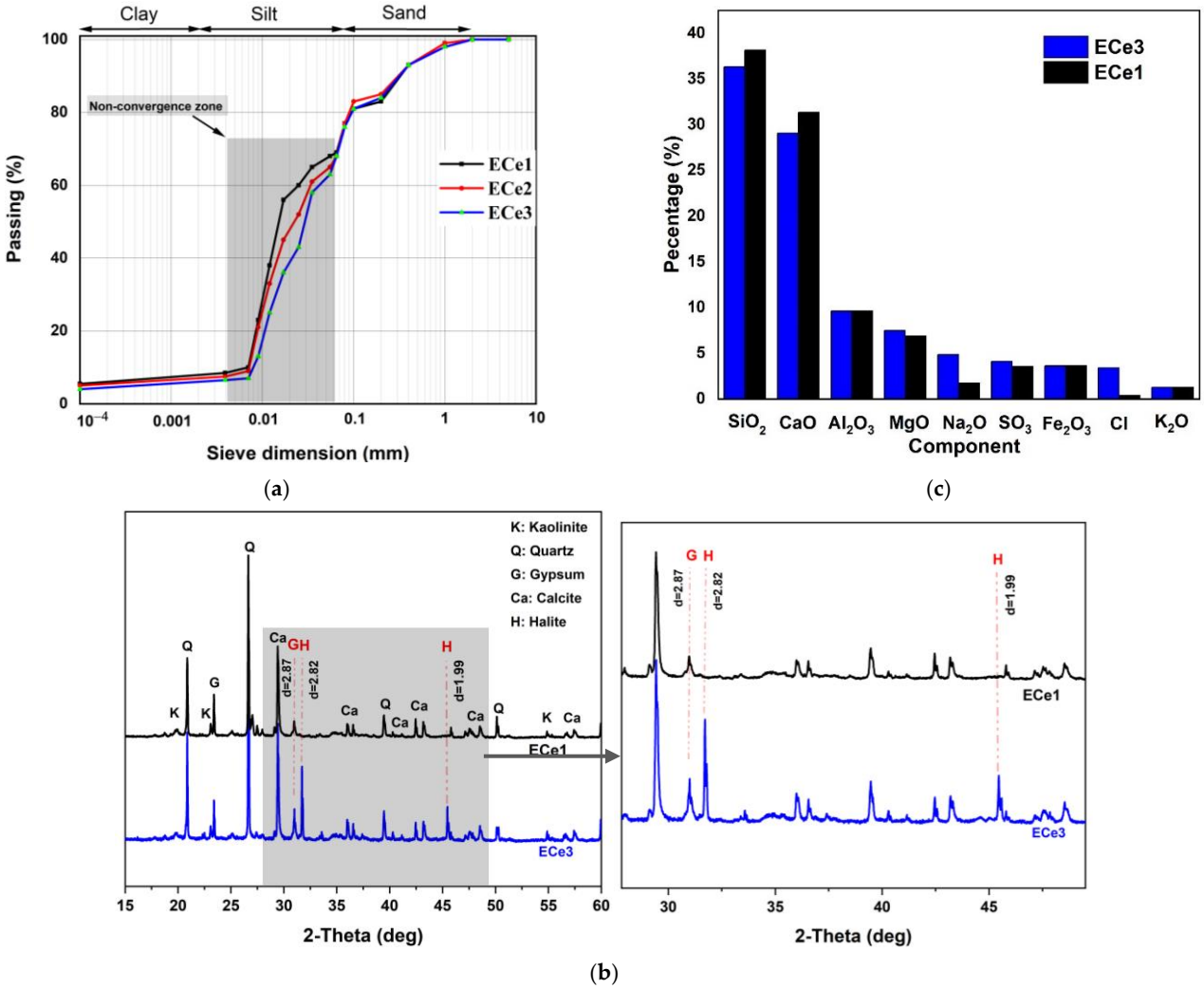

Figure 8. Grain distribution curves of ECe1, ECe2, and ECe3 soils (**a**); mineralogic composition of ECe1 and ECe3 soils by XRD (**b**); chemical composition of ECe1 and ECe3 soils by XRF (**c**).

Figure 8b presents the results of X-ray diffraction (XRD) analysis of soil powders from two soil types, ECe1 and ECe3. The XRD diffractogram of the ECe1 soil revealed the disappearance of two peaks after the leaching process compared with the collected sebkha soil (i.e., ECe3). These two peaks correspond to the halite mineral phases at (2Θ) = 31.7° (d = 2.82°) and (2Θ) = 45.4° (d = 1.99°), respectively. In addition, the ECe1 soil showed a decrease in the size of the gypsum ($CaSO_4$, $2H_2O$) peak at (2Θ) = 31.1° (d = 2.87°), which explains the decrease in the amount of this saline mineral phase. In addition, XRF elemental chemical analysis showed a significant decrease in the quantities of chloride (Cl) and sulfate (SO_3) after washing (Figure 8c). However, this effect was more pronounced for chloride than sulfate, consistently with the XRD results. These results confirm that leaching soluble salts led to a decrease in salinity from ECe = 23.2 $dS.m^{-1}$ to ECe = 2.32 $dS.m^{-1}$, accompanied by the disappearance of halite and a decrease in gypsum. These results confirm those of Hafhouf et al. [18] carried out on the soil of the Ain M'lila sebkha. It could, therefore, be deduced from these results that the variation in the granulometry of the soil as a function of the salinity level for the silty fraction is due to the variation in the quantity of saline mineral phases such as halite and gypsum, which play the role of a natural binder ensuring the bond between the soil grains.

3.3. Effect of Salinity on Untreated Sebkha Soil UCS

Figure 9a shows the stress–strain curves obtained during UCS tests on compacted soil samples at different salinity levels (ECe1, ECe2, and ECe3).

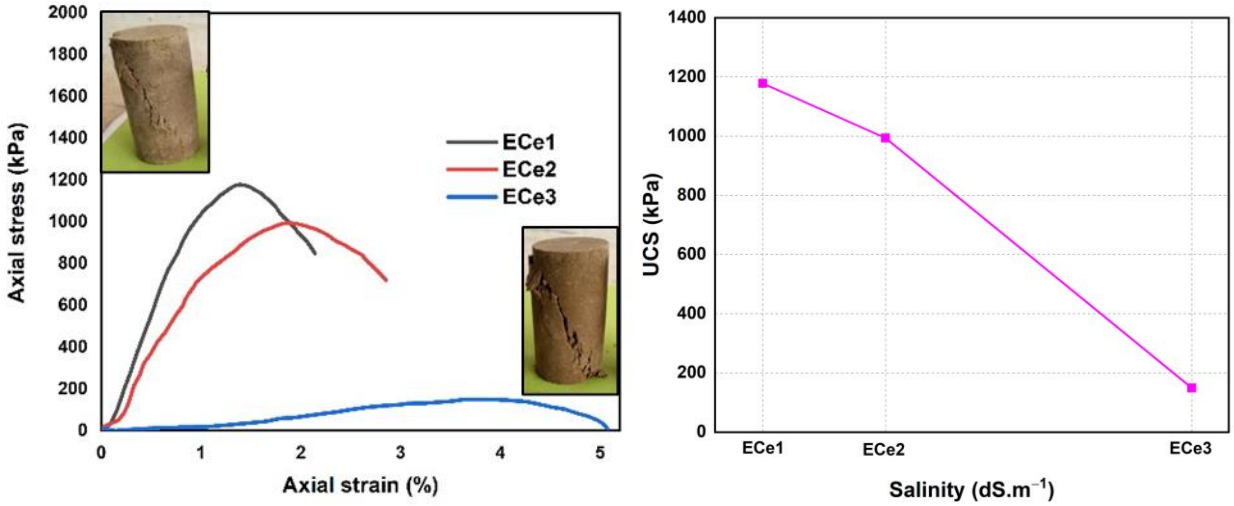

(**a**) (**b**)

Figure 9. Stress–strain curves of ECe1, ECe2, and ECe3 soils (**a**), UCS at different salinity levels (**b**).

These curves show that all the samples exhibited a softening–deformation behavior. The ductile behavior was more pronounced with increasing salinity. For instance, the ECe3 soil did not exhibit a prominent peak, and the strength decreased gradually after failure. Conversely, the stress–strain curve shows a clear peak for the ECe1 soil, with the strength decreasing rapidly. It is crucial to note that the maximum deformation associated with the maximum stress at failure was higher when the latter is low. For example, for the ECe3 soil, its maximum deformation corresponding to rupture and its strength were ε = 3.79% and UCS = 149.8 kPa, respectively, whereas for ECe1 soil, these values were ε = 1.4% and UCS = 1178.9 kPa, respectively. The rate of increase in resistance was 57.06 kPa per unit decrease in salinity when varied from ECe3 to ECe2, whereas it was 29.77 kPa when varied from ECe2 to ECe1 (Figure 9b). However, these curves show that the slope of the segment before fracture increased with decreasing salinity, which explains the increase in soil rigidity with decreasing salinity. This observation is illustrated by the rupture mode of the soil specimens (Figure 8a). The soil with the lowest salinity level, ECe1, had a single large, apparent oblique crack. However, for the soil with the highest salinity level, ECe3, the main oblique crack was preceded by small cracks before rupture, which explains its low rigidity compared with that of ECe1.

It is important to note that, with a specific water content, as the salinity of the soil pore water increases (i.e., salt solution concentration rises), it induces a significant precipitation of crystallized salts. These salts are considered natural cementitious compounds in the soil, which enhances the bonding of soil grains and aggregates, resulting in improved strength [21,37]. However, in the present study, it was found that increasing salinity decreased the strength of the soil tested on a continuous trend. Mineralogical analysis of the Ain M'lila sebkha soil revealed that it was mainly composed of the mineral phases halite (NaCl) and gypsum ($CaSO_4$, $2H_2O$), which were the main cementitious agents in this sebkha soil. After washing the ECe3 soil with D-W, the ECe1 soil was obtained. This latter showed the disappearance of NaCl and a decrease in $CaSO_4$, $2H_2O$. A recent study by Li and Yang [20] examined the influence of water and salt content on soil strength characteristics. The researchers determined that the critical point where a change in strength occurs is when the water content reaches 12%. Beyond this point, increased salt content leads to decreased soil resistance. Moreover, research by Dai et al. [64] showed that the moderate

dissolution rate of $CaSO_4$, $2H_2O$ (0.2%) increases in the presence of other salts, such as NaCl. In the present study, the increase in the dissolution rate of $CaSO_4$, $2H_2O$ in the presence of highly soluble NaCl salt and a relatively high water content of w_{opt} = 11.8% resulted in an overall increase in the total dissolution rate of soluble salt crystals for compacted samples with ECe3 salinity level. In the dry state, part of the solid particles in the soil could be replaced by soluble salt crystals. When these salt crystals dissolved at a higher rate, some salt crystals were transferred to the fluids in the soil, causing a portion of solid particles to disappear. Hence, friction between the soil particles was reduced. This resulted in the dispersion of the soil structure and, ultimately, weakened the soil's resistance. Finally, a reduction in the salinity of Ain M'lila sebkha soil was associated with a reduction in the weak cementitious bonds of minerals such as halite and gypsum, inducing a significant increase in the strength of this soil at its w_{opt}.

These results can be linked to observations in the field. Hot, arid climates with low rainfall and high evaporation rates characterize the lands of the sebkha. When these solute solutions evaporate, they leave behind a crust of white, highly soluble salt, such as halite. This crust forms a hard surface supporting a vehicle [4,65,66]. However, the saline crust's high dissolution, due to its high content of soluble salts such as halite and direct contact with surface rainwater, causes the highly soluble ions to be washed laterally and downward. This process weakens the soil support surface, making it easier for vehicle wheels to get stuck (Figure 10).

Figure 10. Damage caused on sebkha surface by wheels.

In practice, to use this soil as a base for embankments and to make it easy to access and compact the embankments effectively, it is crucial to reduce the salinity of this soil. The resistance of ECe3 soil was significantly reduced at its w_{opt}. It should be noted that this effect is more likely to increase in natural conditions because the w_{ntr} is generally higher than the water (11.8% vs. 18.19%). Therefore, steps should be taken to protect against water exposure or improve this type of soil by binder treatment before starting construction projects.

3.4. Effect of Salinity and Curing Time on Carbonation Content of Sebkha Soil

Figure 11 shows the impact of salinity and curing time on samples' calcium carbonate ($CaCO_3$) content at different salinity levels after lime treatment. The ECe3 soil showed a greater rate of increase in $CaCO_3$ than the ECe2 and ECe1 soils. After treatment, the $CaCO_3$ increased from 41.58% to 47.63% for ECe3, whereas it increased from 43.05% to 47.23% and from 43.51% to 47.33% for ECe2 and ECe1, respectively. This result confirmed the hypothesis mentioned previously that the higher OLC of soil ECe3 was due to the higher precipitation of $CaCO_3$ after adding lime compared with the other soils (i.e., ECe1 and ECe2). Therefore, the higher salt content in the Ain M'lila sebkha soil induced more

significant precipitation of $CaCO_3$ after treatment, requiring more lime to ensure the pozzolanic reaction.

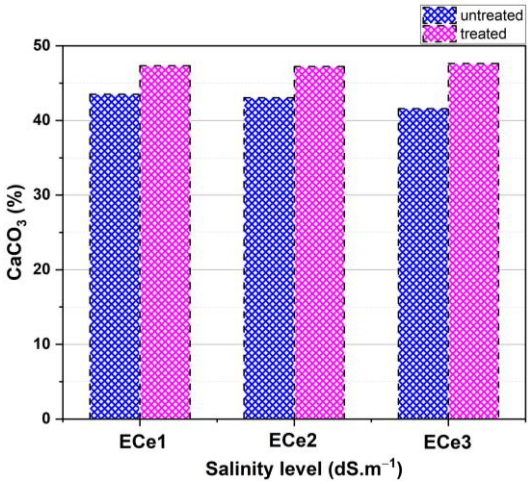

Figure 11. $CaCO_3$ content of untreated and treated ECe1, ECe2, and ECe3 soils by calcimeter.

3.5. Effect of Salinity and Curing Time on Sebkha Soil UCS

Figure 12 illustrates the effect of curing times (0 d, 3 d, 7 d, 14 d, and 28 d) on the stress–strain curves of three saline soil samples treated with lime. These results show that the slope of the stress–strain curves before failure decreased with increasing curing time up to 3 d, after which the slope increased to 28 d of curing. This behavior is distinguished because this slope became more remarkable after 28 curing days than for the untreated soils. However, this behavior was observed only for the ECe1 and ECe2 soils. Notably, the slope increase, which indicates the stiffness of the soil, was higher for the ECe1 soil than the ECe2 soil. However, for the ECe3 soil, the stiffness increased rapidly after 3 d of curing and remained almost constant for up to 28 d. Based on these findings, the addition of lime had a significant impact on the stiffness of the soil during the different curing periods for the ECe1 and ECe2 soils but had a negligible effect on the ECe3 highly saline soil. Regarding the maximum deformations that correspond to failure, it was found that for the ECe3 soil, the maximum deformation that corresponded to failure was influenced by the curing time only from 0 to 3 d because $\varepsilon = 3.79\%$ at 0 d, decreasing to $\varepsilon = 1.28\%$ after 3 d of curing. After this period, the latter remained almost constant with increasing curing time ($\varepsilon = 1.23\%$ vs. $\varepsilon = 1.28\%$). However, for the ECe1 and ECe2 soils, this deformation decreased with increasing curing time. For example, for the ECe1 soil, the value of $\varepsilon = 1.40\%$ at 0 d decreased to $\varepsilon = 1.15\%$ after 28 d of curing.

From these observations, it can be deduced that adding lime reduced these maximum deformations, i.e., increased the brittleness of the treated soil. Regarding maximum failure strength, the ECe3 soil strength increased from 146 kPa in the untreated state to 239 kPa, 255 kPa, and 325 kPa at 3 d, 14 d, and 28 d of curing, respectively. This represents increases of 63.7% from 0 d to 3 d, 6.7% from 3 d to 14 d, and 27.5% from 14 d to 28 d, for a total increase of 36% from 3 d to 28 d of curing. However, the maximum strength for the ECe1 and ECe2 soils decreased by 52.5% and 49.8% from 0 d to 3 d of curing, respectively. After that, for the ECe1 soil, it increased by 42.4% and 116.5% from 3 d to 14 d and from 14 d to 28 d, while it increased by 40.5% and 94.6% for the same periods for the ECe2 soil. Hence, a short curing period of 3 d is considered a critical point for the strength of sebkha soil treated with different salinities. In the ECe1 and ECe2 soils, the strength decreased and then increased until it reaches a value higher than the initial untreated value after 28 d of curing (1178.9 kPa vs. 1723.48 kPa and 1000 kPa vs. 1362.22 kPa).

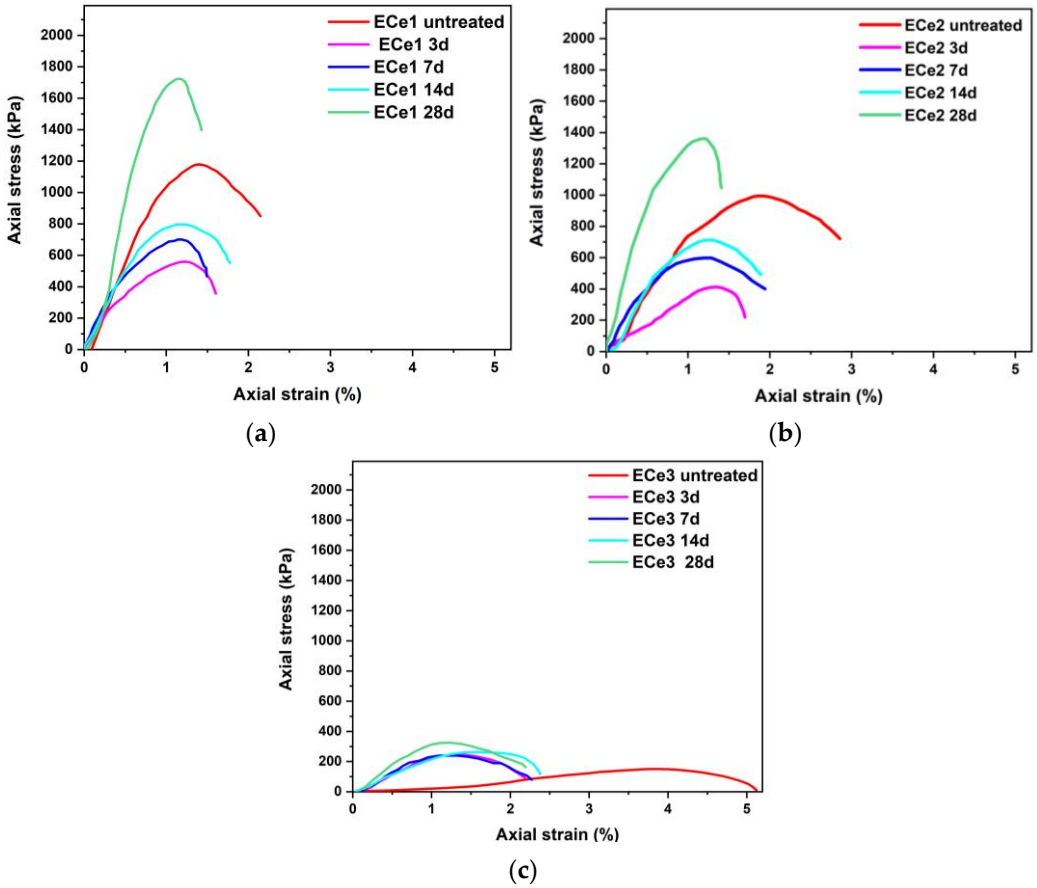

Figure 12. Salinity effects on the stress–strain curves of untreated and lime-treated soils at different curing periods (0 d, 3 d, 7 d, 14 d, and 28 d): (**a**) ECe1 soil, (**b**) ECe2 soil, and (**c**) ECe3 soil.

On the other hand, the strength increased significantly below this point, then increased with a low value for the ECe3 soil. This can be justified by a cation exchange (CE) occurring rapidly after adding lime to the soil–water mixture. However, a study by Mohd and Yunus [67] showed that the dissolution rate of salts in water is faster than that of lime and provided sufficient cations for CE. Therefore, CE in this sebkha soil was strongly related to the cations present in the pore water. These cations can be increased by increasing the amount of binder and the existence of soluble salts. However, in the present study, the intensity of CE in the ECe3 soil was expected to be higher than in the other soils (ECe1 and ECe2) because the ECe3 soil had higher OLC (3% vs. 1.5%) and higher salt content (i.e., halite and gypsum). As a result, the strength of this soil increased significantly from 0 d to 3 d of curing.

Furthermore, mineralogical analysis of ECe1 soil showed a disappearance of halite and a decrease in gypsum. The quantity of gypsum remaining after adding lime and water disrupted the strength of this soil during the curing period. In fact, after mixing the soil with lime and water, primary ettringite appeared rapidly because of the dissolution of gypsum [67,68]. Ettringite is an expansive phase that destroyed the structure of the ECe1 soil. However, this effect was more pronounced in the ECe2 soil, which contained an intermediate salt content, with a higher quantity of gypsum than the ECe1 soil. Therefore, it seems the harmful effect of gypsum in the short term was also linked to its quantity.

Xing et al. [35] found that the presence of Mg^{2+}, Cl^{-}, and SO_4^{2-} ions in a salt-rich soil with cement inhibited the formation of cementitious compounds. The present study's findings are supported by the lack of strength improvement in the ECe3 treated soil, which was attributed to the harmful effects of chloride and sulfate salts in the soil. The increase in strength also confirmed this, as salinity was reduced in the ECe1 and ECe2 soils. Hence,

in the present study, the high concentration of vulnerable ions in the pore water between ECe3 soil particles with low clay fraction enhanced their capacity to coat finer particles and limited their exposure to lime hydration. As a result, coating the finer particles, these ions prevented them from being exposed to lime hydration, disrupting the formation of hydration products and interfering with strength development.

Finally, it can be deduced that the low clay fraction and the high salinity are two factors that affected the resistance of the originally collected ECe3 soil. The high salinity resulted in the high ion content present in the interstitial water that enveloped the fine particles, slowing the pozzolanic reaction on the one hand. Since these ions are also directly related to the clay fraction, their existence in small quantities did not allow a normal pozzolanic reaction between the lime and the mineral phases, disturbing the strength of the ECe3 soil.

3.6. Effect of Salinity on the Mineralogy of Cured Soils

After 28 days of curing, powders of the untreated and lime-treated soils were analyzed by X-ray diffraction for two types of soil, ECe1 and ECe3 (Figure 13a,b), and variations in the diffractograms were observed. In the lime-treated ECe3 soil, the mineralogical composition did not change after 28 days of curing. In addition, the mineral salt phases remained essentially constant during the curing process, indicating that these minerals did not participate in the hydration reaction.

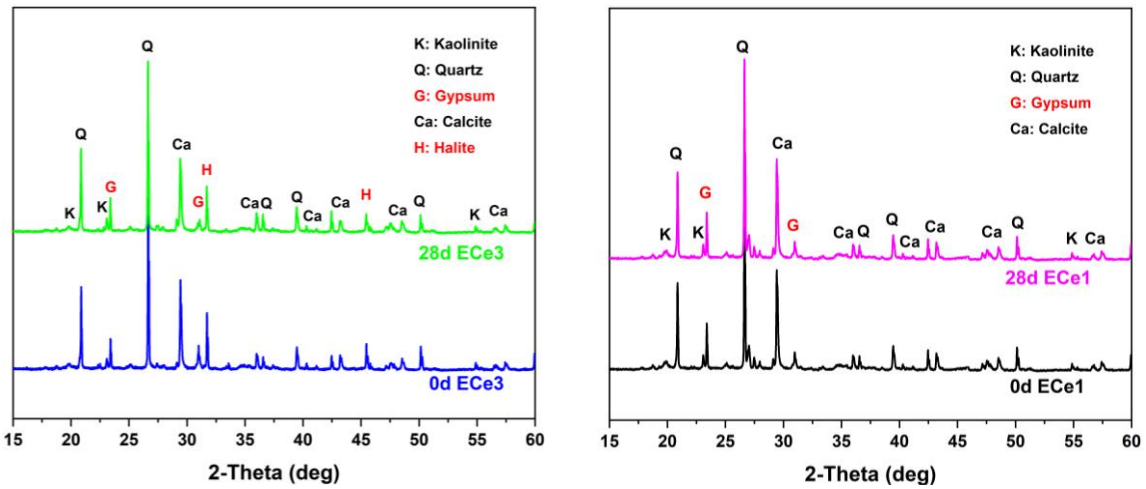

Figure 13. Mineralogy composition by XRD of untreated and treated soil samples: (**a**) ECe3 soil and (**b**) ECe1 soil.

On the other hand, no new peaks corresponding to cementitious products (CAH and CSH) were observed for the ECe1 soil. However, the ECe1 soil's strength increased with curing time. As the XRD results showed no significant change in the mineralogical composition of lime-treated samples at different salinity levels, thermal analyses (TGA) (Figure 14a) were also carried out. The results obtained show that the untreated ECe3 and ECe1 soil powders had mass losses of 2.92% and 2.29%, respectively, between 100 °C and 200 °C, indicating dehydration of the water molecules constituting the gypsum (Figure 14b). Furthermore, mass losses of 16.95% and 17.78% for the ECe3 and ECe1 soil, respectively, were observed between 650 °C and 750 °C, indicating decomposition/decarbonization of the calcite (Figure 14c). In addition, mass losses between 800 °C and 1100 °C were noted with values of 8.89% and 0.98% for ECe3 and ECe1 soil, respectively, corresponding to the melting phase of halite (Figure 14d). These results are consistent with previous results, which indicated the disappearance of halite, diminution of gypsum, and increase of calcite for ECe1 soil compared with ECe3 soil.

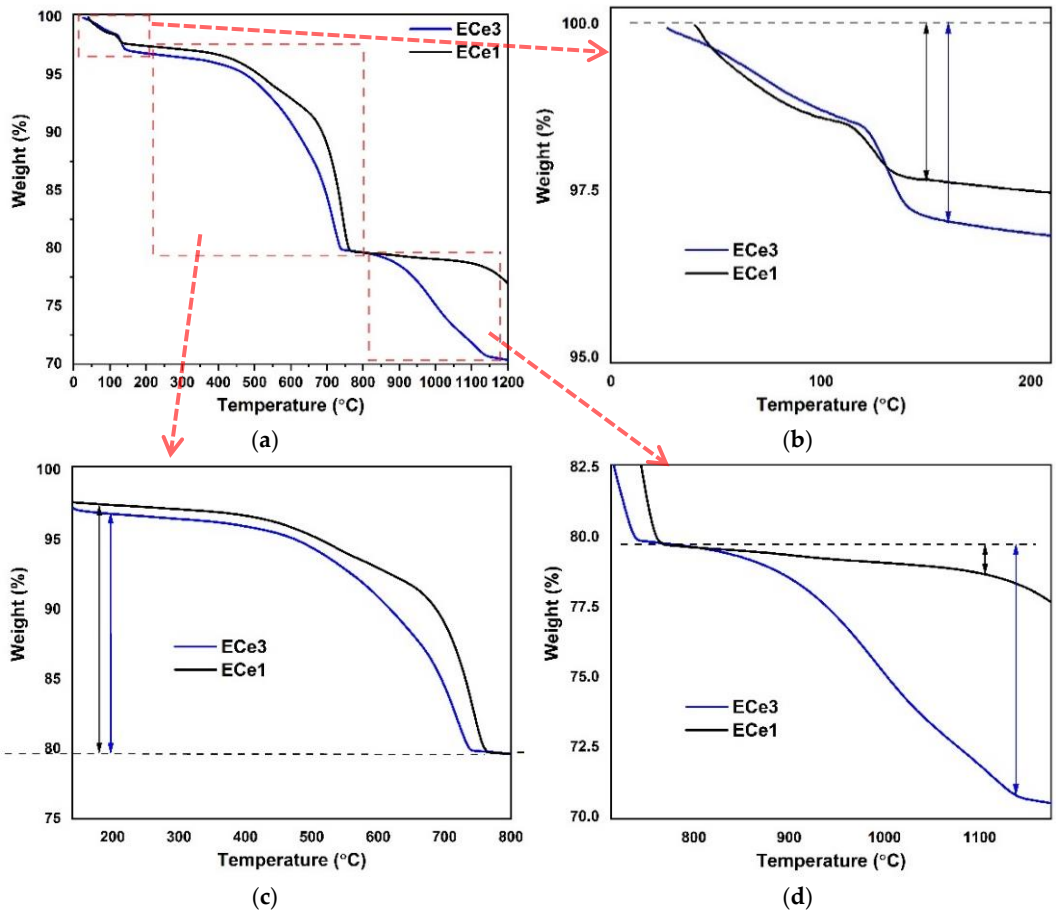

Figure 14. Loss of mass by TGA of untreated ECe3 and ECe1 soils (**a**); dehydration of gypsum (**b**), decomposition of calcite (**c**), and melting of halite (**d**).

However, the ECe1 and ECe3 treated samples showed the formation of a new mineral phase, portlandite, represented by a loss of mass illustrated between 400 °C and 500 °C (Figure 15a,b). The losses of this phase were 1.5% and 1.2% for the ECe1 and ECe3 soils, respectively (Figure 15c). It should be noted that the OLC in the ECe3 soil was higher than that in the ECe1 soil (3% vs. 1.5%), although the results obtained for the content of portlandite developed were inverse, indicating that the saline phases had a detrimental effect on the lime hydration process. However, the XRD tests did not detect this phase, because the portlandite was in the amorphous state or because of the detection limit of the physicochemical equipment (i.e., the quantity to be measured with only 1.5% and 3% lime treatment). Nevertheless, this amorphous phase is considered a cementitious compound that increased the bridges and strengthened the adhesion between soil particles, thus improving the mechanical behavior of ECe1 soil [11].

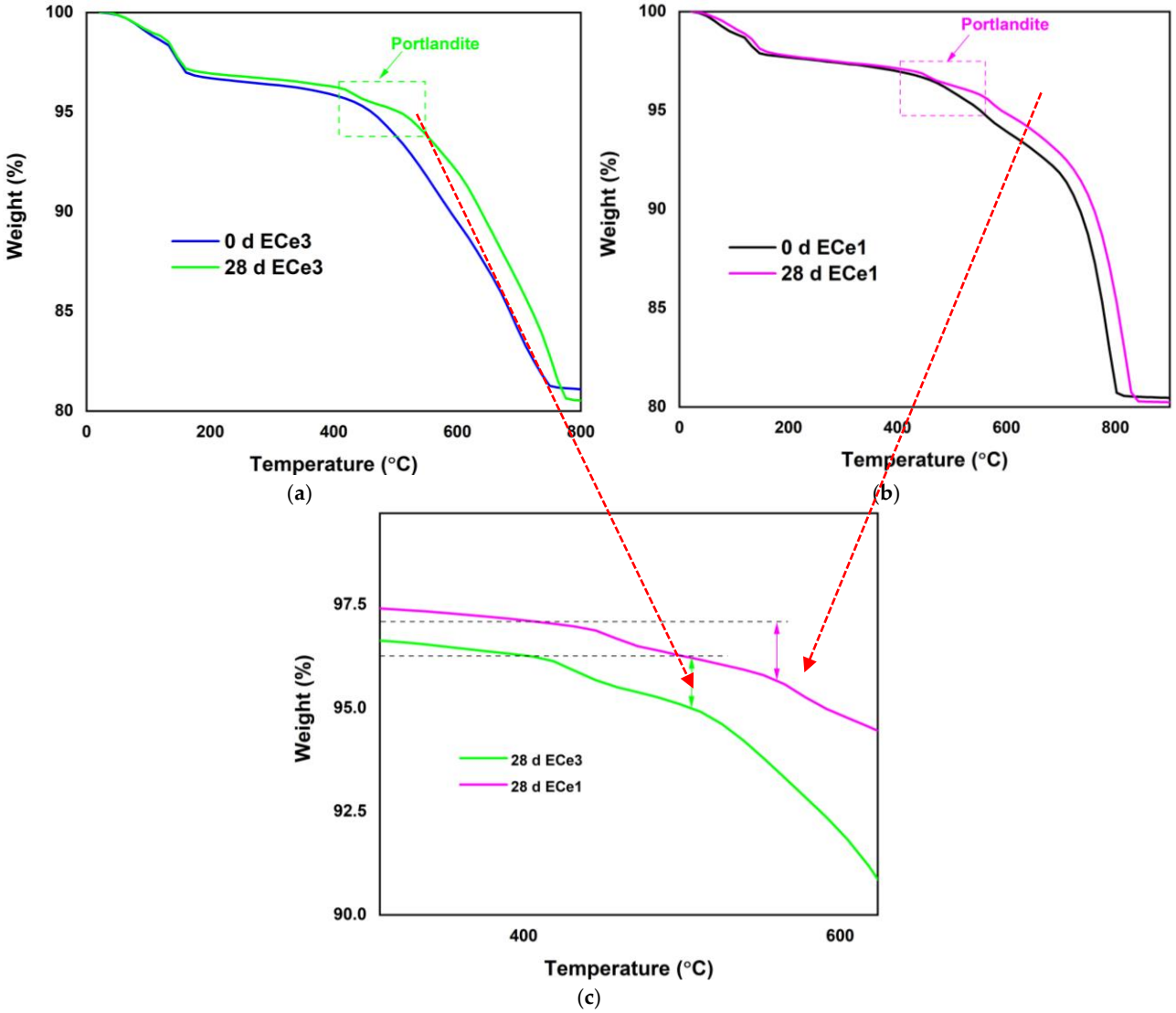

Figure 15. Losses of mass by TGA of untreated and treated ECe3 (**a**) and ECe1 (**b**) soils and dehydration of portlandite (**c**).

4. Conclusions

This study examined the impact of salinity on the physicochemical and mechanical properties of untreated and air lime-treated sebkha soils from Ain M'lila. To this end, an experimental program, comprising physicochemical and mechanical tests, was carried out on a soil tested originally (ECe3) and after washing to provide samples with medium (ECe2) and low (ECe1) salinity. The results of this program showed a significant effect of salinity on the tested soil resistance. The conclusions of this work can be cited as follows:

- A higher soil salinity required greater incorporation of lime to achieve acceptable performance. This incorporation reached 1.5% for the ECe1 soil and 3% for the ECe3 soil. This difference was due to the consumption of OH^- and Ca^{2+} ions, present in the saline interstitial solution, by Mg^{2+} and HCO^{3-} ions, leading to the precipitation of Mg $(OH)_2$ and $CaCO_3$.
- Salinity significantly impacted the shape of the particle size curve, particularly on the silty fraction. The reduction in salinity was linked to a decrease in gypsum content and the total disappearance of halite, which minimized the cementation of aggregates. Consequently, more fine particles were observed in the ECe1 soil, with an 18% increase in fine particles less than 20 μm in diameter.

- For untreated soil, salinity affected $CaCO_3$ precipitation. The latter decreased with increasing salinity. The ECe3 soil contained a large amount of gypsum ($CaSO_4$, $2H_2O$) and, as it contained almost 1/3 CaO of its total mass, more calcium cations (Ca^{2+}) were captured by the sulfate anions ($SO_4{}^{2-}$), resulting in a decrease in $CaCO_3$ compared with the ECe2 and ECe1 soils. However, for the treated soil, the precipitation of $CaCO_3$ was higher in the ECe3 soil than in the ECe2 and ECe1 soils. This was probably due to the reaction of HCO^{3-}, Ca^{2+}, and OH^- ions leading to the precipitation of $CaCO_3$.
- Unconfined compressive strength (UCS) for untreated soil increased when salinity decreased. In fact, in the presence of halite and relatively high w_{opt} of 11.8%, gypsum dissolution was accelerated, thus reducing the number of solid particles and leading to a significant decrease in the UCS of the ECe3 soil. However, in the case of lime-treated soil, since a highly saline environment characterized the ECe3 soil, the $SO_4{}^{2-}$ and Cl^- ions present in the pore water probably covered the low clay fraction, thus disturbing the mechanical strength of the ECe3 soil.
- For treated saline soils, the participation of gypsum and halite was not observed in the formation of cementitious compounds in the ECe3 soil, as shown by the results of the XRD analyses, and no new peaks corresponding to cementitious compounds were detected for either ECe1 or ECe3 soils. However, thermogravimetric analysis (TGA) showed the presence of portlandite. This latter phase was higher in the ECe1 soil than in the ECe3 soil, despite the latter containing a higher lime content than the ECe1 soil. This indicates the negative effect of soluble salts on the strength of the ECe3 soil (natural sebkha soil from Ain M'lila) after lime treatment.

In conclusion, improving the resistance of highly saline soils similar to the Ain M'lila sebkha soil with the addition of lime may be insufficient. However, identifying the season when the sebkha has lower salinity can be beneficial from a technical, economic, and environmental point of view. Lime treating saline soils when they have lower salinity (whenever it is possible) increases their resistance and reduces the optimal quantity of lime to use. However, if the soil contains a low clay fraction, which plays a vital role in the hydration and formation of cementitious compounds, it may be helpful to enrich the soil with pozzolanic fractions such as silica-rich dune sand. Further studies on the optimization of performance of saline soils can also be helpful to increase the use of these soils as building materials for earthen construction, as saline earth is currently rejected and not used for building.

Author Contributions: Data curation, formal analysis, investigation, and methodology: I.B., A.D., I.H., A.M. (Abdelghani Merdas) and A.M. (Adberrahim Meguellati); writing—original draft: I.B., A.D., I.H., A.M. (Abdelghani Merdas) and A.M. (Adberrahim Meguellati); writing—review and editing: I.B., I.H. and P.F. All authors have read and agreed to the published version of the manuscript.

Funding: This research received no external funding.

Data Availability Statement: The data presented in this study are available on request from the corresponding author.

Acknowledgments: The last author acknowledges the support of the research unit CERIS–Civil Engineering Research and Innovation for Sustainability (DOI: 10.54499/UIDB/04625/2020). The authors would like to thank the LTPEst SETIF laboratory for granting them access to conduct part of the experimental program.

Conflicts of Interest: The authors declare no conflict of interest.

References

1. Liu, Y.; Wang, Q.; Liu, S.; ShangGuan, Y.; Fu, H.; Ma, B.; Chen, H.; Yuan, X. Experimental Investigation of the Geotechnical Properties and Microstructure of Lime-Stabilized Saline Soils under Freeze-Thaw Cycling. *Cold Reg. Sci. Technol.* **2019**, *161*, 32–42. [CrossRef]
2. Alshenawy, A.O.; Hamid, W.M.; Alnuaim, A.M. A Review on the Characteristics of Sabkha Soils in the Arabian Gulf Region. *Arab. J. Geosci.* **2021**, *14*, 2018. [CrossRef]

3. Youssef, A.M.; Maerz, N.H. Overview of Some Geological Hazards in the Saudi Arabia. *Env. Earth Sci.* **2013**, *70*, 3115–3130. [CrossRef]
4. Moayed, R.Z.; Izadi, E.; Heidari, S. Stabilization of Saline Silty Sand Using Lime and Micro Silica. *J. Cent. S. Univ.* **2012**, *19*, 3006–3011. [CrossRef]
5. Zhao, X.; Shen, A.; Guo, Y.; Li, P.; Lv, Z. Pavement Mechanic Response of Sulfate Saline Soil Subgrade Section Based on Fluid–Structure Interaction Model. *Int. J. Pavement Res. Technol.* **2017**, *10*, 497–506. [CrossRef]
6. Al-Homidy, A.A.; Dahim, M.H.; Abd El Aal, A.K. Improvement of Geotechnical Properties of Sabkha Soil Utilizing Cement Kiln Dust. *J. Rock. Mech. Geotech. Eng.* **2017**, *9*, 749–760. [CrossRef]
7. Nu, N.T.; Duong, N.T.; Son, B.T.; Thinh, P.H. Investigation of Salt, Alum Content in Soft Soils and Their Effects on Soil Properties: Case Study in Coastal Areas of Vietnam. *Iraqi Geol. J.* **2020**, *53*, 19–34. [CrossRef]
8. Shen, J.; Wang, Q.; Chen, Y.; Zhang, X.; Han, Y.; Liu, Y. Experimental Investigation into the Salinity Effect on the Physicomechanical Properties of Carbonate Saline Soil. *J. Rock. Mech. Geotech. Eng.* **2024**, *16*, 1883–1895. [CrossRef]
9. Spagnoli, G.; Sridharan, A.; Oreste, P.; Di Matteo, L. A Probabilistic Approach for the Assessment of the Influence of the Dielectric Constant of Pore Fluids on the Liquid Limit of Smectite and Kaolinite. *Appl. Clay Sci.* **2017**, *145*, 37–43. [CrossRef]
10. Tang, S.; She, D.; Wang, H. Effect of Salinity on Soil Structure and Soil Hydraulic Characteristics. *Can. J. Soil. Sci.* **2021**, *101*, 62–73. [CrossRef]
11. Ying, Z.; Cui, Y.-J.; Duc, M.; Benahmed, N. Effect of Salt Solution on the Optimum Lime Contents of Bentonite and Silt. *Acta Geotech.* **2022**, *17*, 3731–3745. [CrossRef]
12. Yang, X.H.; Zhang, S.S.; Liu, W.; Yu, Z.L. Research progress on engineering properties of coarse-grained saline soil. *Jiaotong Yunshu Gongcheng Xuebao/J. Traffic Transp. Eng.* **2020**, *20*, 22–40. [CrossRef]
13. Velde, B.B.; Meunier, A. *The Origin of Clay Minerals in Soils and Weathered Rocks*; Springer Science & Business Media: Berlin/Heidelberg, Germany, 2008.
14. Mohammed, M.S.; Abdullah, E.J. Heavy Metals Pollution Assessment of the Soil in the Northern Site of East Baghdad Oil Field, Iraq. *Iraqi J. Sci.* **2016**, *57*, 175–183.
15. Rodrigues, C.M.; Bio, A.; Amat, F.; Vieira, N. Artisanal Salt Production in Aveiro/Portugal—An Ecofriendly Process. *Saline Syst.* **2011**, *7*, 3. [CrossRef]
16. Faria, P.; Beckett, C.T.S.; Fabbri, A.; Keita, E.; Morel, J.-C.; Perlot, C.; Perrot, A. RILEM Contribution to Earthen Building. In *Second RILEM International Conference on Earthen Construction*; Beckett, C., Bras, A., Fabbri, A., Keita, E., Perlot, C., Perrot, A., Eds.; RILEM Bookseries; Springer Nature Switzerland: Cham, Switzerland, 2024; Volume 52, pp. 194–205; ISBN 978-3-031-62689-0.
17. Gallipoli, D.; Bruno, A.W.; Perlot, C.; Mendes, J. A Geotechnical Perspective of Raw Earth Building. *Acta Geotech.* **2017**, *12*, 463–478. [CrossRef]
18. Hafhouf, I.; Bahloul, O.; Abbeche, K. Effects of Drying-Wetting Cycles on the Salinity and the Mechanical Behavior of Sebkha Soils. A Case Study from Ain M'Lila, Algeria. *CATENA* **2022**, *212*, 106099. [CrossRef]
19. Ying, Z.; Cui, Y.-J.; Benahmed, N.; Duc, M. Investigating the Salinity Effect on Water Retention Property and Microstructure Changes along Water Retention Curves for Lime-Treated Soil. *Constr. Build. Mater.* **2021**, *303*, 124564. [CrossRef]
20. Li, H.; Yang, M. Study on Unconfined Compressive Strength and Deformation Characteristics of Chlorine Saline Soil. *Sci. Rep.* **2024**, *14*, 1478. [CrossRef]
21. Zhang, S.; Yang, X.; Xie, S.; Yin, P. Experimental Study on Improving the Engineering Properties of Coarse Grain Sulphate Saline Soils with Inorganic Materials. *Cold Reg. Sci. Technol.* **2020**, *170*, 102909. [CrossRef]
22. Aiban, S.; Al-Ahmadi, H.; Asi, I.; Siddique, Z.; Al-Amoudi, O.S.B. Effect of Geotextile and Cement on the Performance of Sabkha Subgrade. *Build. Environ.* **2006**, *41*, 807–820. [CrossRef]
23. Yu, X.; Dan, H.-C.; Xin, P. Method for Improving Leaching Efficiency of Coastal Subsurface Drainage Systems. *J. Irrig. Drain. Eng.* **2018**, *144*, 04018019. [CrossRef]
24. Negi, A.S.; Faizan, M.; Siddharth, D.P.; Singh, R. Soil Stabilization Using Lime. *Int. J. Innov. Res. Sci. Eng. Technol.* **2013**, *2*, 448–453.
25. Dhar, S.; Hussain, M. The Strength and Microstructural Behavior of Lime Stabilized Subgrade Soil in Road Construction. *Int. J. Geotech. Eng.* **2021**, *15*, 471–483. [CrossRef]
26. Di Sante, M.; Di Buò, B.; Fratalocchi, E.; Länsivaara, T. Lime Treatment of a Soft Sensitive Clay: A Sustainable Reuse Option. *Geosciences* **2020**, *10*, 182. [CrossRef]
27. Eades, J.L.; Grim, R.E. *A Quick Test to Determine Lime Requirements for Lime Stabilization*; Highway Research Board: Washington, DC, USA, 1966; pp. 61–72.
28. Emarah, D.A.; Seleem, S.A. Swelling Soils Treatment Using Lime and Sea Water for Roads Construction. *Alex. Eng. J.* **2018**, *57*, 2357–2365. [CrossRef]
29. Li, M.; Chai, S.X.; Zhang, H.Y.; Du, H.P.; Wei, L. Feasibility of Saline Soil Reinforced with Treated Wheat Straw and Lime. *Soils Found.* **2012**, *52*, 228–238. [CrossRef]
30. Pei, W.; Shouxi, C. Laboratory AND in-situ tests on solidified saline soils for highway fillings. *J. Eng. Geol.* **2011**, *19*, 440–446.
31. Jiang, Y.; Dai, H.; Fisonga, M.; Li, C.; Hong, Z.; Xia, C.; Deng, Y. Feasibility and Mechanism of High Alumina Cement-Modified Chlorine Saline Soil as Subgrade Material. *Constr. Build. Mater.* **2024**, *429*, 136411. [CrossRef]
32. Wei, L.; Chai, S.; Wang, P. Mechanical Properties of Stabilized Saline Soil as Road Embankment Filling Material. *Geomech. Eng.* **2024**, *37*, 499–510.

33. Koslanant, S. Influence of Storage Conditions on Geotechnical Properties of Ariake Clay and on Its Chemical Stabilization. Ph.D. Thesis, Saga University Graduate School of Science and Engineering, Saga, Japan, 2006.
34. Zhang, D.; Cao, Z.; Fan, L.; Liu, S.; Liu, W. Evaluation of the Influence of Salt Concentration on Cement Stabilized Clay by Electrical Resistivity Measurement Method. *Eng. Geol.* **2014**, *170*, 80–88. [CrossRef]
35. Xing, H.; Yang, X.; Xu, C.; Ye, G. Strength Characteristics and Mechanisms of Salt-Rich Soil–Cement. *Eng. Geol.* **2009**, *103*, 33–38. [CrossRef]
36. Aldaood, A.; Bouasker, M.; Al-Mukhtar, M. Impact of Freeze–Thaw Cycles on Mechanical Behaviour of Lime Stabilized Gypseous Soils. *Cold Reg. Sci. Technol.* **2014**, *99*, 38–45. [CrossRef]
37. Li, M.; Chai, S.; Du, H.; Wang, C. Effect of Chlorine Salt on the Physical and Mechanical Properties of Inshore Saline Soil Treated with Lime. *Soils Found.* **2016**, *56*, 327–335. [CrossRef]
38. Cuisinier, O.; Le Borgne, T.; Deneele, D.; Masrouri, F. Quantification of the Effects of Nitrates, Phosphates and Chlorides on Soil Stabilization with Lime and Cement. *Eng. Geol.* **2011**, *117*, 229–235. [CrossRef]
39. Carteret, R.D.; Buzzi, O.; Fityus, S.; Liu, X. Effect of Naturally Occurring Salts on Tensile and Shear Strength of Sealed Granular Road Pavements. *J. Mater. Civ. Eng.* **2014**, *26*, 04014010. [CrossRef]
40. Khadka, S.D.; Jayawickrama, P.W.; Senadheera, S.; Segvic, B. Stabilization of Highly Expansive Soils Containing Sulfate Using Metakaolin and Fly Ash Based Geopolymer Modified with Lime and Gypsum. *Transp. Geotech.* **2020**, *23*, 100327. [CrossRef]
41. Rica, H.C.; Saussaye, L.; Boutouil, M.; Leleyter, L.; Baraud, F. Stabilization of a Silty Soil: Effects of Disruptive Salts. *Eng. Geol.* **2016**, *208*, 191–197. [CrossRef]
42. Nie, Y.; Ni, W.; Lü, X.; Tuo, W. Exploring the Mechanical Behavior and Microstructure of Compacted Loess Subjected to Dry-Wet Cycles and Chemical Contamination. *J. Rock. Mech. Geotech. Eng.* **2024**, *16*, 3673–3695. [CrossRef]
43. Zhang, F.; Wang, G.; Kamai, T.; Chen, W.; Zhang, D.; Yang, J. Undrained Shear Behavior of Loess Saturated with Different Concentrations of Sodium Chloride Solution. *Eng. Geol.* **2013**, *155*, 69–79. [CrossRef]
44. Ouadah-Bedidi, Z.; Vallin, J. Fertility and Population Policy in Algeria: Discrepancies between Planning and Outcomes. *Popul. Dev. Rev.* **2013**, *38*, 179–196. [CrossRef]
45. Koull, N.; Chehma, A.; Guezzoun, N.; Hamouda, N.; Bellahcene, O. Qualité Des Eaux Des Zones Humides Du Bas Sahara Algérien. *Rev. Des Bioressources* **2016**, *6*, 113–124. [CrossRef]
46. Amarouayache, M.; Derbal, F.; Kara, M.H. Caractéristiques Écologiques et Biologiques d'Artemia Salina (Crustacé, Anostracé) de La Sebkha Ez-Zemoul, Algérie Nord-Est. *Rev. D'écologie (La Terre La Vie)* **2010**, *65*, 129–138. [CrossRef]
47. *NF P94-093*; Determination of the Compaction Characteristics of a Soil—Standards Proctor Test—Modified Proctor Test. AFNOR: Paris, France, 1999.
48. United States Department of Agriculture (USDA). *Soil Mechanics Level I. Module 3–USDA Textural Soil Classification Study Guide*; USDA: Washington, DC, USA, 1987.
49. *NF P94-077*; Uniaxial Compressive Test. AFNOR: Paris, France, 1997.
50. *NF P94-050*; Determination of Moisture Content. Oven Drying Method. AFNOR: Paris, France, 1995.
51. *NF P94-056*; Granulometric Analysis—Dry Sieving Method after Washing. AFNOR: Paris, France, 1996.
52. *NF P94-057*; Granulometric Analysis—Hydrometer Methodle. AFNOR: Paris, France, 1992.
53. *ASTM D4318-17e1*; Standard Test Methods for Liquid Limit, Plastic Limit, and Plasticity Index of Soils. ASTM International: West Conshohocken, PA, USA, 2018.
54. *ASTM D2487-17*; Standard Practice for Classification of Soils for Engineering Purposes (Unified Soil Classification System). ASTM international: West Conshohocken, PA, USA, 2017.
55. *NF P94-048*; Determination of the Carbonate Content—Calcimeter Method. AFNOR: Paris, France, 1996.
56. Richards, A.L. *Diagnosis and Improvement of Saline and Alkali Soils*; US Department of Agriculture: Washington, DC, USA, 1954.
57. Loyer, J.-Y. Classification Des Sols Salés: Les Sols Salic. *Cah. ORSTOM Série Pédologie* **1991**, *61*, 51–61.
58. Thomas, G.W. Soil pH and Soil Acidity. In *SSSA Book Series*; Sparks, D.L., Page, A.L., Helmke, P.A., Loeppert, R.H., Soltanpour, P.N., Tabatabai, M.A., Johnston, C.T., Sumner, M.E., Eds.; Soil Science Society of America, American Society of Agronomy: Madison, WI, USA, 2018; pp. 475–490; ISBN 978-0-89118-866-7.
59. Al-Mukhtar, M.; Lasledj, A.; Alcover, J.-F. Behaviour and Mineralogy Changes in Lime-Treated Expansive Soil at 20 C. *Appl. Clay Sci.* **2010**, *50*, 191–198. [CrossRef]
60. Di Sante, M.; Fratalocchi, E.; Mazzieri, F.; Pasqualini, E. Time of Reactions in a Lime Treated Clayey Soil and Influence of Curing Conditions on Its Microstructure and Behaviour. *Appl. Clay Sci.* **2014**, *99*, 100–109. [CrossRef]
61. Negawo, W.J.; Di Emidio, G.; Bezuijen, A.; Verastegui Flores, R.D.; François, B. Lime-Stabilisation of High Plasticity Swelling Clay from Ethiopia. *Eur. J. Environ. Civ. Eng.* **2019**, *23*, 504–514. [CrossRef]
62. Pansu, M.; Gautheyrou, J. *Handbook of Soil Analysis*; Springer: Berlin/Heidelberg, Germany, 2006; ISBN 978-3-540-31210-9.
63. Klein, C.; Hurlbut, C.S., Jr. *Manual of Mineralogy*; John Wiley and Sons: Hoboken, NJ, USA, 1985.
64. Dai, Z.; Kan, A.T.; Shi, W.; Zhang, N.; Zhang, F.; Yan, F.; Bhandari, N.; Zhang, Z.; Liu, Y.; Ruan, G.; et al. Solubility Measurements and Predictions of Gypsum, Anhydrite, and Calcite Over Wide Ranges of Temperature, Pressure, and Ionic Strength with Mixed Electrolytes. *Rock. Mech. Rock. Eng.* **2017**, *50*, 327–339. [CrossRef]
65. Glennie, K.W. *Desert Sedimentary Environments*; Elsevier: Amsterdam, The Netherlands, 2010.

66. Akili, W.; Ahmed, N. The Sabkhas of Eastern Saudi Arabia: Geotechnical Considerations. In Proceedings of the First Saudi Engineering Conference, Jaddah, Saudi Arabia, 14–19 May 1983; pp. 300–322.
67. Mohd Yunus, N.Z.; Wanatowski, D.; Marto, A.; Jusoh, S.N. Strength Improvement of Lime-Treated Clay with Sodium Chloride. *Geotech. Res.* **2017**, *4*, 192–202. [CrossRef]
68. Rajasekaran, G. Sulphate attack and ettringite formation in the lime and cement stabilized marine clays. *Ocean Eng.* **2005**, *32*, 1133–1159. [CrossRef]

Disclaimer/Publisher's Note: The statements, opinions and data contained in all publications are solely those of the individual author(s) and contributor(s) and not of MDPI and/or the editor(s). MDPI and/or the editor(s) disclaim responsibility for any injury to people or property resulting from any ideas, methods, instructions or products referred to in the content.